

Giant Vesicles Containing Magnetic Nanoparticles and Quantum Dots: Feasibility and Tracking by Fiber Confocal Fluorescence Microscopy**

Grégory Beaune, Benoit Dubertret, Olivier Clément, Catherine Vayssettes, Valérie Cabuil, and Christine Ménager*

Magnetic nanoparticles (MNPs) are currently being investigated because of their numerous applications in the biological field,^[1] in particular, for their use as contrast agents in magnetic resonance imaging (MRI)^[2] and as biological labels.^[3] Recently, the production of hybrid materials that contain both iron oxide nanoparticles and quantum dots (QDs) was explored.^[4,5] However, their applications are limited because of the difficulty in encapsulating both organic-soluble QDs and water-soluble MNPs.^[6] In this context, vesicles are particularly attractive, as they are readily synthesized, biocompatible, and biodegradable. They can co-encapsulate hydrophobic molecules within the phospholipid bilayer, and hydrophilic species in the vesicle interior. Encapsulation protects the loaded species against degradation by the surrounding biological medium and reduces their toxic effects. Vogel et al. have recently described the insertion of QDs in the lipid bilayer of giant vesicles.^[7] Some of us have described the encapsulation of MNPs inside vesicles and the possibility of guiding them with a magnetic force in vitro and in vivo.^[8,9] Here, we report a new strategy that uses emulsion processes to encapsulate two types of nanoparticles. In the present study, MNPs and QDs, which exhibit unique optical properties, are entrapped in vesicles. The combination of MRI and optical techniques represents a complementary imaging pair with potential clinical utility. MRI offers the ability to follow the distribution of molecules in vivo or provide anatomical reference, whereas optical techniques can be applied to obtain detailed information at the subcellular level.

Figure 1 depicts the two routes followed to produce magnetic and fluorescent vesicles, referred to in the following as hybrid vesicles (HVs). Both processes start from a water-in-oil emulsion, the oil phase being a dispersion of CdSe/ZnS

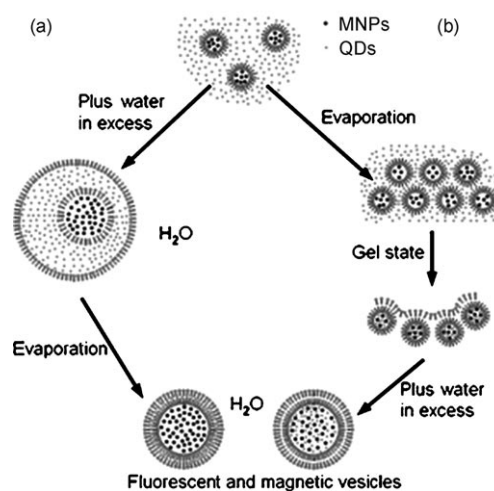


Figure 1. Outline of the preparation of HVs by a) a multiple emulsion (ME) process and b) reverse-phase evaporation (REV).

QDs coated with a mixture of tri-*n*-octylphosphine (TOP) and tri-*n*-octylphosphine oxide (TOPO), and the aqueous phase a pH 7 dispersion of citrate-coated maghemite nanoparticles (γ -Fe₂O₃). For the multiple emulsion (ME) process, the intermediate stage is the formation of emulsions, whereas it is a gel state for the reverse-phase evaporation (REV) method. We investigated two different surfactants: didodecylmethylammonium bromide (DDAB)^[9] and dioleoylphosphatidylcholine (DOPC). DDAB is a synthetic surfactant with two hydrophobic tails that forms bilayers in water and DOPC is a classical phospholipid.

Optical microscopy images of vesicles are shown in Figure 2. The HVs appeared to be strongly magnetic and fluorescent. When the magnetic field is removed, the alignment of the vesicles is broken and they disperse again within a few seconds. The HVs are spherical with a diameter ranging from 0.1 to 10 μ m and a broad Gaussian distribution of diameters. The average diameter, for both DDAB and DOPC HVs, is 2 μ m with a polydispersity $\sigma = 0.3$. Then, by comparing fluorescence microscopy images without or under a magnetic field, it was found that a great proportion of the vesicles were both magnetic and fluorescent (Figure 2a and b).

[*] G. Beaune, Prof. V. Cabuil, Dr. C. Ménager
UPMC/CNRS/ESPCI
Laboratoire des Liquides Ioniques et Interfaces Chargées UMR 7612
équipe Colloïdes Inorganiques (LI2C)
Université Paris 6 (UPMC) Bat F(74), case 63
4 place Jussieu, 75252 Paris Cedex 05 (France)
Fax: (+33) 1-44-27-36-75
E-mail: menager@ccr.jussieu.fr
Dr. B. Dubertret
UPR 5, Laboratoire d'Optique Physique
ESPCI
10 rue Vauquelin, 75231 Paris Cedex 05 (France)
Prof. O. Clément, Dr. C. Vayssettes
Laboratoire de Recherche en Imagerie (LRI) EA 4062
Université Paris Descartes
156 rue de Vaugirard, 75015 Paris (France)

[**] We thank Aude Michel (LI2C) for support with electron microscopy, Lucy Sengmanivong (PF-ICT IFR65) for confocal studies, Delphine Talbot (LI2C) for chemical analyses, and Gwennael Autret (LRI) for assistance with the Cellvizio device.

Supporting information for this article is available on the WWW under <http://www.angewandte.org> or from the author.

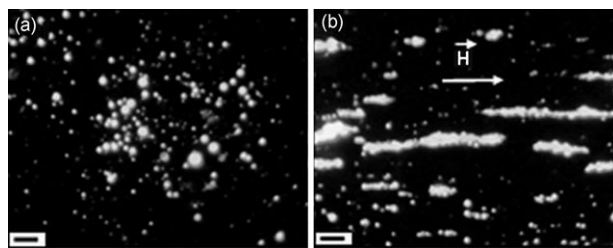


Figure 2. Fluorescence images of vesicles synthesized by the ME process with DDAB: a) without magnetic field, b) under a magnetic field of $H = 48 \text{ kA m}^{-1}$. Scale bars: $10 \mu\text{m}$.

The magnetic susceptibilities of the HVs were measured by magnetophoresis experiments.^[10] The high susceptibilities obtained, 0.1 for the ME process and 0.2 for the REV process (volume fractions $\varphi = 0.8$ and 1.6% , respectively), indicate an efficient encapsulation of the magnetic particles, which was confirmed by transmission electron microscopy (TEM; Figure 3). Note that the shape of the magnetization curve (see the Supporting Information) is the same as that for the initial magnetic fluid, which indicates that the magnetic behavior of the latter is not modified by encapsulation.

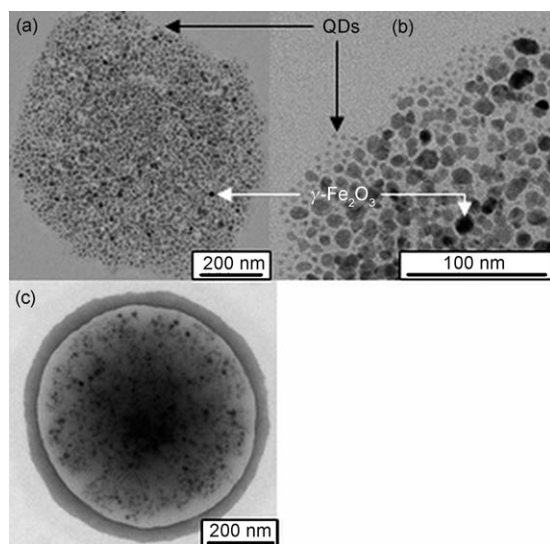


Figure 3. TEM images of vesicles synthesized with a,b) DOPC by REV and c) DDAB (stained) by the ME process.

The photostability of QDs is very sensitive to the environment. Depending on the solvent, the photobleaching of QDs can occur in a few minutes (for example, in ether/cyclohexane). Here, HVs observed by fluorescence microscopy appear very bright and are resistant to photobleaching over a period of several hours (Figure 4).

As a result of the evaporation of the samples on the grid, we cannot draw conclusions from the TEM images on the location of the two kinds of particles in the HVs. ME synthesis was observed by optical microscopy. The water-in-oil emulsion appears as brown droplets, which correspond to the

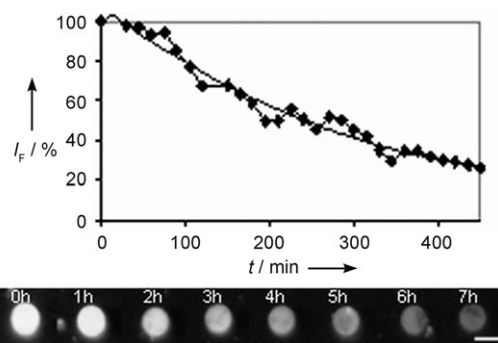


Figure 4. Photobleaching test (100-W Hg lamp). Decrease of the fluorescence intensity with time for magnetic and fluorescent vesicles synthesized by the ME process with DDAB. Scale bar: $10 \mu\text{m}$.

aqueous magnetic dispersion in the cyclohexane/QD organic phase (Figure 5a). In multiple emulsions, the magnetic droplets appear brown in the transmission mode and black in the fluorescence mode, and can be distinguished from the

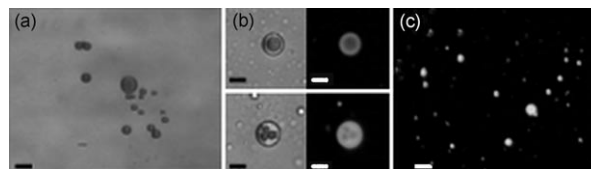


Figure 5. Optical microscopy in the transmission and fluorescence modes. a) Water-in-oil emulsions, b) multiple emulsions, and c) vesicles. Scale bars: $10 \mu\text{m}$.

fluorescent zones as slightly colored in transmission mode and green in fluorescence mode (Figure 5b). These observations are in agreement with the formation of a core-shell structure where the dots are localized inside the membrane. After evaporation of the organic phase, the fluorescence seems homogeneously distributed in the whole structure (Figure 5c), but confocal cross sections of vesicles led to a readily assignable fluorescence distribution (Figure 6). This result shows that the process used to synthesize HVs allows control of the QD distribution in the vesicle: fluorescence was found at the level of the membrane (inside or on) for HVs produced by the ME process, as expected, whereas DDAB and DOPC vesicles produced by REV were fluorescent in the bulk. As a matter of fact, during the ME process, the removal of the organic solvent from the emulsions resulted in the incorporation of QDs into the bilayer. This insertion was possible

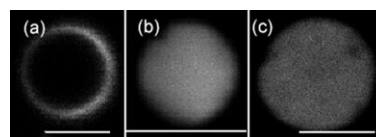


Figure 6. Confocal fluorescence cross-sectional image of HVs made of: a) DDAB by the ME process, b) DDAB by the REV process, c) DOPC by the REV process. Scale bars: $7.5 \mu\text{m}$.

because the size of the QDs (3 nm) was less than the thickness of the membrane. As concerns the REV process, it is well-known^[11] that formation of the intermediate gel state brings about the collapse of the aqueous droplets. The result is co-encapsulation of the MNPs and QDs in the aqueous core of the vesicles.

HVs stored at 6°C remained stable for more than six months for DDAB and two months for DOPC without noticeable aggregation or morphological modifications.

In vivo experiments were performed to test the non-toxicity, blood circulation, and biodistribution of the HVs. The in vitro and in vivo imaging applications of these HVs were investigated with a recently developed device that combines confocal fluorescence microscopy with an optical-fiber miniprobe (0.3 mm diameter), which collects light from the observation site and conveys it toward a specific imaging device. This so-called Cellvizio device enables in vivo, in situ, microvascular exploration and imaging of intact organs in their native environment, with limited invasiveness and preservation of the physiological state of the tissues.^[12]

In vitro tests showed that the movements of HVs (whatever the synthesis procedure) under the action of a magnetic force (external magnet) are readily detectable with this apparatus. The HVs were concentrated magnetically and the probe was introduced directly into the solution of vesicles (Figure 7).

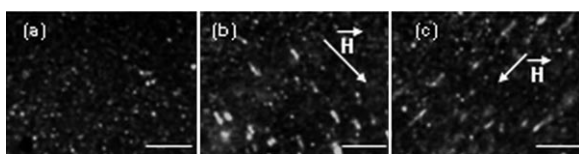


Figure 7. Cellvizio pictures of an in vitro test performed with vesicles synthesized by the REV process: a) without and b,c) with a magnetic field. Scale bars: 100 μm .

All in vivo experiments complied with French legislation, ethical principles, and guidelines for experiments on animals. The concentration of iron injected was 0.9 mg g^{-1} body weight, far below the acute toxic dose for mice (50 mg g^{-1} , intravenous). Clear results on the toxicity of QDs are not available. However, studies using lipid-coated QDs did not show toxic effects on cells,^[6,13] and some in vivo studies on mice showed no toxicity until 133 days.^[14] In our system, the toxicity of QDs is limited by the presence of a ZnS layer protecting the CdSe core, and by their encapsulation inside vesicles. Furthermore, the QDs were used at a very low concentration with injections of 7 pmol g^{-1} body weight.

The probe was maintained in contact with the surface of the organs while the tissues were regularly hydrated with a saline buffer (physiological serum; 0.9% NaCl). After injection, fluorescent HVs were quickly and clearly detected in the kidney, spleen, liver, and heart (Figure 8), and HVs showed the vascular architecture of the heart and lungs. These experiments are very promising, because the fluorescence intensity obtained is very high and it is the first visualization of QDs with the Cellvizio device. The tests were only

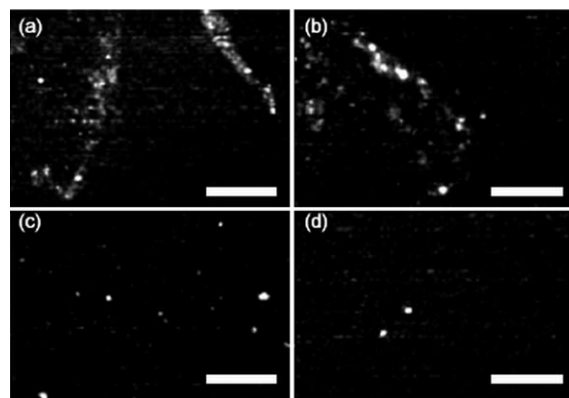


Figure 8. Cellvizio pictures of in vivo experiments in the a) heart, b) lungs, c) liver, and d) spleen of mice. Scale bars: 100 μm .

preliminary because the micrometer-sized HVs could have a limited circulation in the blood vessels. Magnetic and fluorescent small unilamellar vesicles (SUVs) are currently developed.

In conclusion, a novel hybrid system made of hydrophilic MNPs and hydrophobic fluorescent nanoparticles encapsulated in giant vesicles has been developed. The location of the QDs appeared to be controlled by the synthesis process. The system exhibited both strong magnetic properties and low photobleaching characteristics. We demonstrated the feasibility of using it for in vitro and in vivo applications, and are now investigating the yield of this promising system at the nanometer scale to improve in vivo applications, such as magnetic guidance of HVs to tumors and possible uses of these materials for hyperthermia treatment.

Experimental Section

1,2-Dioleoyl-*sn*-glycero-3-phosphocholine (DOPC) and didodecyltrimethylammonium bromide (DDAB) were purchased from Sigma and Fluka, respectively.

Synthesis of maghemite nanoparticles: 1) According to a procedure already described, superparamagnetic $\gamma\text{-Fe}_2\text{O}_3$ (maghemite) nanocrystals were prepared by alkaline co-precipitation of FeCl_2 and FeCl_3 salts.^[15] Polydisperse $\gamma\text{-Fe}_2\text{O}_3$ nanocrystals were synthesized by oxidizing magnetite (1.3 mol) in nitric acid (2N, 1 L) containing iron nitrate (1.3 mol) with boiling. 2) Citrated ferrofluid: After decantation/sieving, the maghemite particles were heated at 80°C for 30 min in water, then supplemented with sodium citrate (70 g) before precipitation in acetone at 25°C. The final iron content was checked by flame spectrometry. The recovered magnetic fluid was ready to use and stable at room temperature for years.

Synthesis of CdSe/ZnS nanoparticles: Core-shell CdSe/ZnS QDs with 3 nm diameter were synthesized based on an established method.^[16] They emit with a maximum around 525 nm and were dispersed in cyclohexane. The QDs were coated with a mixture of TOP and TOPO (see the Supporting Information).

Preparation of HVs: 1) REV process: A solution (0.5 μM , 5 mL) of QDs suspended in cyclohexane was mixed with surfactant (DOPC or DDAB, 13 mg). Then a solution of maghemite (400 μL ; $[\text{Fe}] = 75 \text{ mM}$) was added. A water-in-oil emulsion was obtained by sonication in a bath for 2 min. The cyclohexane was evaporated for 3 min using a Rotavapor. The thin vesicle films obtained were then dispersed in distilled water (5 mL). 2) ME process: The oil phase was a solution (1.25 mL, 2 μM) of QDs suspended in cyclohexane; DDAB

(2% by weight) was solubilized in this phase. The magnetic fluid (20 μ L, [Fe] = 3 M) was added to the oil phase at room temperature and an emulsion was obtained by using a vortex (20 s). The emulsion (0.75 mL) was quickly introduced into distilled water (15 mL). Then, the cyclohexane was evaporated at 45–50 °C under a nitrogen stream over a period of 30 min.

All TEM images were obtained by using a JEOL 100 CX instrument (100 kV). Negative staining was performed with a solution of uranyl acetate (2% by weight) for DDAB samples and ammonium molybdate (2% by weight) for DOPC vesicles.^[11] Optical microscopy images were observed by using a Leica microscope (\times 40, NA 0.65, 100-W Hg lamp), with pictures taken by a CCD camera and digitized on a computer. All confocal images were recorded by using a Leica TCS SP2 confocal microscope with an excitation wavelength of 488 nm. The Cellvizio device (Mauna Kea Technologies, France) uses a 488-nm laser source and collection over a range of 500–650 nm.

Received: February 8, 2007

Revised: April 26, 2007

Published online: June 11, 2007

Keywords: fluorescence · nanoparticles · organic–inorganic hybrid composites · quantum dots · vesicles

-
- [1] S. Mornet, S. Vasseur, F. Grasset, E. Duguet, *J. Mater. Chem.* **2004**, *14*, 2161–2175.
 [2] R. Weissleder, A. Moore, U. Mahmood, R. Bhorade, H. Benveniste, E. A. Chiocca, J. P. Bacion, *Nat. Med.* **2000**, *6*, 351–355.

- [3] a) F. Bertorelle, C. Wilhelm, J. Roger, F. Gazeau, C. Ménager, V. Cabuil, *Langmuir* **2006**, *22*, 5385–5391; b) L. A. Perrin-Cocon, P. N. Marche, C. L. Villiers, *Biochem. J.* **1999**, *338*, 123–130.
 [4] a) N. Gaponik, I. L. Radtchenko, G. B. Sukhorukov, A. L. Rogach, *Langmuir* **2004**, *20*, 1449–1452.
 [5] a) D. Wang, J. He, N. Rosenzweig, Z. Rosenzweig, *Nano Lett.* **2004**, *4*, 409–413; b) G. P. Wang, E. Q. Song, H. Y. Xie, Z. L. Zhang, Z. Q. Tian, C. Zuo, D. W. Pang, D. C. Wu, Y. B. Shi, *Chem. Commun.* **2005**, 4276–4278.
 [6] S. K. Mandal, N. Lequeux, B. Rotenberg, M. Tramier, J. Fattaccioli, J. Bibette, B. Dubertret, *Langmuir* **2005**, *21*, 4175–4179.
 [7] G. Gopalakrishnan, C. Danelon, P. Izewska, M. Prummer, Y. Bolinger, I. Geissbühler, D. Demurtas, J. Dubochet, H. Vogel, *Angew. Chem.* **2006**, *118*, 5604–5609; *Angew. Chem. Int. Ed.* **2006**, *45*, 5478–5483.
 [8] J. P. Fortin-Ripoche, M. S. Martina, C. Wilhelm, C. Ménager, S. Lesieur, F. Gazeau, O. Clément, *Radiology* **2006**, *239*, 415–424.
 [9] C. Ménager, V. Cabuil, *Colloid Polym. Sci.* **1994**, *272*, 1295–1299.
 [10] O. Sandre, C. Ménager, J. Prost, V. Cabuil, J. C. Bacri, A. Cebers, *Phys. Rev. E* **2000**, *62*, 3865–3870.
 [11] R. R. C. New in *Liposomes: A Practical Approach* (Eds.: D. Rickwood, B. D. Hames), IRL Press, **1990**, p. 140.
 [12] E. Laemmel, M. Genet, G. Le Goualher, A. Perchant, J. F. Le Gargasson, E. Vicaut, *J. Vasc. Res.* **2004**, *41*, 400–411.
 [13] B. Dubertret, P. Skourides, D. J. Norris, V. Noireaux, A. H. Brivanlou, A. Libchaber, *Science* **2002**, *298*, 1759–1762.
 [14] R. Hardman, *Environ. Health Perspect.* **2006**, *114*, 165–172.
 [15] R. Massart, *IEEE Trans. Magn.* **1981**, *17*, 1247–1248.
 [16] D. V. Talapin, A. L. Rogach, A. Kornowski, M. Haase, H. Weller, *Nano Lett.* **2001**, *1*, 207–211.